International Conference on Space Optics—ICSO 2018

Chania, Greece

9–12 October 2018

Edited by Zoran Sodnik, Nikos Karafolas, and Bruno Cugny

Optical metrology terminal for satellite-to-satellite laser ranging

Oliver Mandel

Michael Chwalla

Thilo Schuldt

Jasper Krauser

et al.

International Conference on Space Optics — ICSO 2018, edited by Zoran Sodnik, Nikos Karafolas, Bruno Cugny, Proc. of SPIE Vol. 11180, 1118049 · © 2018 ESA and CNES · CCC code: 0277-786X/18/$18 · doi: 10.1117/12.2536072

Optical metrology terminal for satellite-to-satellite laser ranging

Oliver Mandel*[ab], Michael Chwalla[a], Thilo Schuldt[bc], Jasper Krauser[a], Dennis Weise[a], and Claus Braxmaier[bc]
[a]Airbus Defence and Space GmbH, Claude-Dornier-Str., 88090 Immenstaad, Germany; [b]Center of Applied Space Technology and Microgravity (ZARM), University of Bremen, Am Fallturm 2, 28359 Bremen, Germany; [c]Institute of Space Systems, German Aerospace Center (DLR), Robert-Hooke-Str. 7, 28359 Bremen, Germany

ABSTRACT

Interferometric laser ranging is an enabling technology for high-precision satellite-to-satellite tracking within the context of earth observation, gravitational wave detection, or formation flying. In orbit, the measurement system is affected by environmental influences, particularly satellite attitude jitter and temperature fluctuations, demanding an instrument design, which has a high level of thermal stability and is insensitive to rotations around the satellite's center of mass. Different design approaches for a heterodyne dynamic laser ranging instrument have been combined to a new improved design concept that involves the inherent beam tracking capabilities of a retroreflector into a mono-axial configuration with nanometer accuracy. In order to facilitate the accommodation onboard a future satellite mission, the design allows for a continuously adjustable flexible phase center position. To cover large inter-spacecraft distances, the instrument design comprises an active transponder system, featuring a two-dimensional beam steering mechanism to align a local, strong laser to the (weak) input beam without affecting the measurement path.

To this end, a dynamic laser ranging instrument is presented, which has compact dimensions and is fully integrated on a single Zerodur baseplate. The instrument performance will be evaluated in a dedicated test setup providing a flat-top beam simulating the laser beam received from a distant spacecraft, including a beam steering subsystem, which allows for monitoring of pathlength variations when the angle of incidence at the optical instrument is changing.

Keywords: Satellite-to-Satellite tracking, laser interferometry, metrology, retroreflector, tilt-to-piston coupling, beam steering, differential wavefront sensing

1. INTRODUCTION

Since its launch in March 2002, the Gravity Recovery And Climate Experiment (GRACE) provided a precise map of temporal variations in the Earth's mass distribution and gravity field. Shortly after its decommissioning in 2017/18, the successor mission GRACE Follow-On was launched in order to continue the measurements. Unlike in other geodetic missions, the measurement principle of GRACE does not rely on the transmission of electromagnetic signals through the atmosphere. Instead, the distance between the two separated spacecraft in a low-earth orbit is affected when the constellation is traversing anomalies in Earth's gravity field and measured by means of a microwave ranging instrument. In addition, GRACE Follow-On is equipped with a laser interferometer as a technology demonstrator increasing the accuracy from a few microns into the few 10 nanometer regime [1].

For future (gravity) missions new instrument architectures are investigated. Several studies have already been carried out in this context such as e/e^2-motion [2,3] and NG2 [4], deriving mission requirements and providing enhanced optical instrument designs. In terms of ranging accuracy, the future gravitational wave observatory Laser Interferometer Space Antenna (LISA) necessitates an improvement of three orders of magnitude and therefore requires a different instrument architecture, however, several design and manufacturing approaches investigated during the extensive LISA research are also equally valid for a future gravity mission.

In addition, an instrument design that allows to measure absolute distances while not relying on a large inter-spacecraft distance would enable formation flying, e.g. using several spacecraft in order to synthesize for example a large optical aperture, investigated within the DARWIN mission concept.

*oliver.mandel@airbus.com; phone +49 7545 8 2414; airbus.com

2. OPTICAL INSTRUMENT

2.1 Performance Goals and Requirements

The achievable measurement performance of a future gravity mission does not rely entirely on the ranging accuracy, since all non-gravitational forces acting on the spacecraft have to be measured separately and compensated for. The largest noise contribution to the ranging signal is caused by laser frequency noise due to an unequal arm length in the interferometer. For next generation gravity missions (NGGM), 1064 nm laser sources are under development with a frequency stability of better than 40 Hz/√Hz by means of an optical cavity [3]. At a distance of 300 km this corresponds to a ranging noise of 43 nm/√Hz. A second crucial noise source referred to as tilt-to-piston coupling must be taken into account and minimized by instrument design in order to avoid the coupling of residual spacecraft jitter into the measurement signal. Therefore, the optical instrument may be mounted with the point of minimal coupling aligned to the spacecraft's center of mass. This is typically the point where a high precision accelerometer for the measurement of non-gravitational influences is mounted. Other noise sources such as temperature variations, pointing errors, imperfections of the optical instrument and noise from the measurement system increase the noise budget for the overall ranging accuracy to about 50 nm/√Hz, as given in Table 1. In order to keep the required laser power at a moderate level, a transponder system using a local laser source on each spacecraft is part of the optical instrument presented here.

Table 1. Performance goals and expected environmental influences

Inter-spacecraft distance	50 - 300	km
Spacecraft attitude jitter	100	µrad/√Hz
Measurement band	1 - 200	mHz
Temperature stability	4	mK/√Hz
Ranging accuracy	50	nm/√Hz
Field of regard	5	mrad
Mechanical clearance around reference point	> 15	cm

2.2 Optical Design

In the context of GRACE Follow-On and NGGM, several instrument designs have been published, which use either a large retroreflector in a racetrack configuration [1] or demand a sophisticated beam pointing system [2]. The retroreflector based approaches have two particular properties, which make them attractive for this kind of instrument. First, the reflected beam remains always aligned anti-parallel with respect to the incident beam. Second, the bi-axial nature of the retroreflector offers enough space for an accelerometer placed into its reference point. However, this clearance is geometrically coupled to the offset between the incident and reflected beam and therefore the overall dimensions of the retroreflector.

In an on-axis system, the laser beams are propagating directly along the line-of-sight, requiring only one opening to the outside of the spacecraft. Therefore, in principle two different on-axis instruments are able to work together, whereas bi-axial instruments particularly at short distances requires identical beam offsets and is sensitive to relative roll motions. Since the enclosed area between the beams becomes zero for an on-axis instrument, measurement errors due to the Sagnac effect, especially in pendulum orbits, are avoided. The major drawback so far has been the lack of a simple beam regeneration and pointing scheme that is not part of the measurement path. As an alternative, spacecraft pointing has been proposed in the past [2], demanding attitude and orbit control up to the precision required by the optical link.

The presented optical metrology terminal (OMT) combines both approaches into a new improved design concept that combines the inherent beam tracking capabilities of a retroreflector with a mono-axial configuration. The aperture of a retroreflector and its effect on a laser beam can be significantly altered when additional mirrors are added to the design, according to the corresponding patent application [5]: A single flat mirror in front of the retroreflector allows separating the point of minimal coupling from the retroreflector location (Figure 1-1). With two parallel mirrors, the beam offset of the external beams can be adjusted independently of the retroreflector size, so that a small retroreflector seems equivalent to a larger one (Figure 1-2). The internal beam offset and size of the retroreflector is chosen to be so small, that the beam has just enough clearance to the nearest mirror edges in order to maintain an excellent wavefront quality. However, instead of imitating a larger retroreflector, the external beam offset is minimized and the first mirror replaced with a

beam splitter (Figure 1-3). The glass transmission through the beam splitter has a significant impact on the location of the point of minimal coupling, primarily invoking a longitudinal offset. Polarization optics is used in order to prevent light to be lost at the beam splitter and avoid interference. Although this design concept describes an on-axis system, the bi-axial beam guidance used internally allows utilizing the transponder scheme developed for GRACE Follow-On.

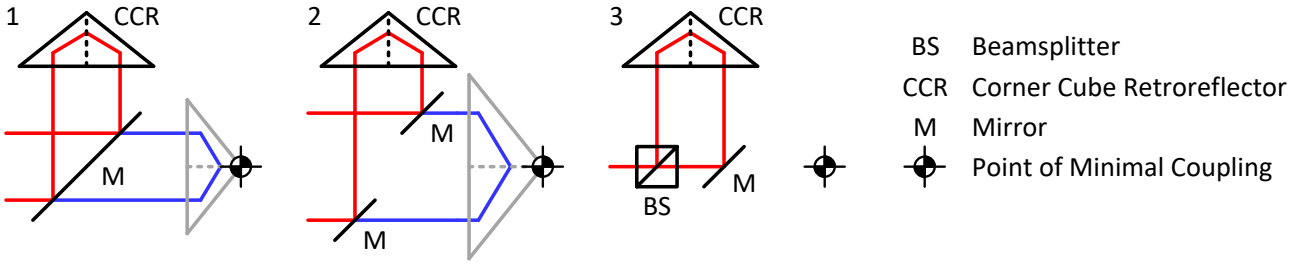

Figure 1, Design concept for the optical instrument

Based on this concept, an entire optical instrument has been designed for potential use in future gravity missions, comprising a compact corner cube retroreflector, a two-dimensional steering mirror, polarization dependent beam separation, a magnifying pupil imaging system and an (optional) acquisition sensor. The instrument design is depicted in Figure 2. The received beam shown in red in Figure 2 is arriving perpendicularly to the baseplate close to its center. The pupil plane is located at half of the roundtrip pathlength, which actually is an optical copy of the signal at the point of minimal coupling from below the baseplate directly on the line-of-sight. The steering mirror, which aligns the transmitted laser beam, has exactly the same distance to the following beam splitter as the pupil plane so that both can be imaged onto two quadrant photodetectors. A magnification factor of 1/9 is used to increase the signal power at the photodetectors by matching the beam size to the active area.

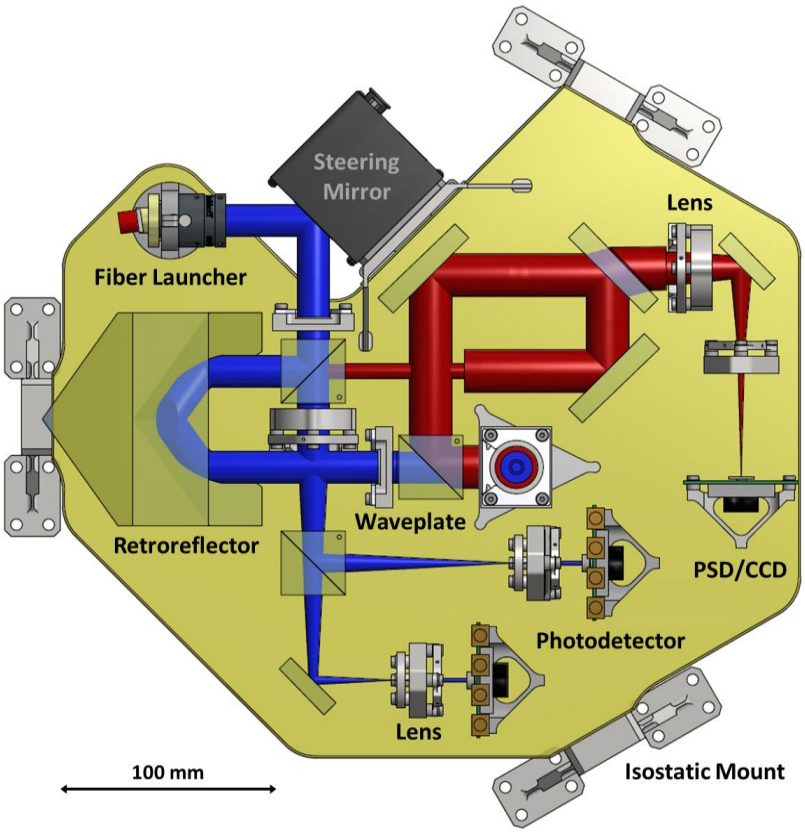

Figure 2, Design of the optical instrument with all components mounted onto a single baseplate.

The photodetectors measure the phase difference and a relative tilt between both beams by means of differential wavefront sensing [1, 6]. This signal is used for closed loop control of the steering mirror. The major part of the local beam continues the path of the received beam, is reflected at the retroreflector, and leaves the instrument back towards the distant spacecraft. During initial link acquisition the narrow laser beams are aligned towards the remote spacecraft, e.g. following a multi-dimensional scan pattern. The acquisition sensor located on the right side of the instrument in Figure 2 detects the angle of incidence of the received beam in order to reduce the time required to establish the link. The full measurement path contains flat optical surfaces only. The instrument design provides a flexible adjustment of the location of the point of minimal coupling simplifying spacecraft accommodation in a future mission. Further, the conveniently large field of regard does not demand a sophisticated attitude control system while a fast steering mirror with light movable mass is compensating for spacecraft jitter.

During measurements, the instrument will be affected by temperature variations causing thermal expansion and shifts of the refractive index. The total measurement path inside the optical instrument has a length of about 75 cm. In order to keep the resulting error in the range of a few nanometers, the baseplate material must have a coefficient of thermal expansion in the order of 10^{-6}/K or below. Since this value is barely achievable with metal, a Zerodur baseplate is used instead having margin by two orders of magnitude. The same material choice has already been made for the optical bench in LISA pathfinder and, therefore, is a flight proven technology. Three metal feet made of Invar are bonded to the edges of the baseplate for isostatic mounting of the instrument to the satellite structure.

2.3 Assembly status

The assembly of the optical instrument is currently in progress. A positioning template has been designed in order to fix the noncritical optical components to the baseplate (Figure 3). A two component epoxy resin is used to adhesively bond the components together. Previous tests have shown that this method is a viable option for space-borne optical instruments [7].

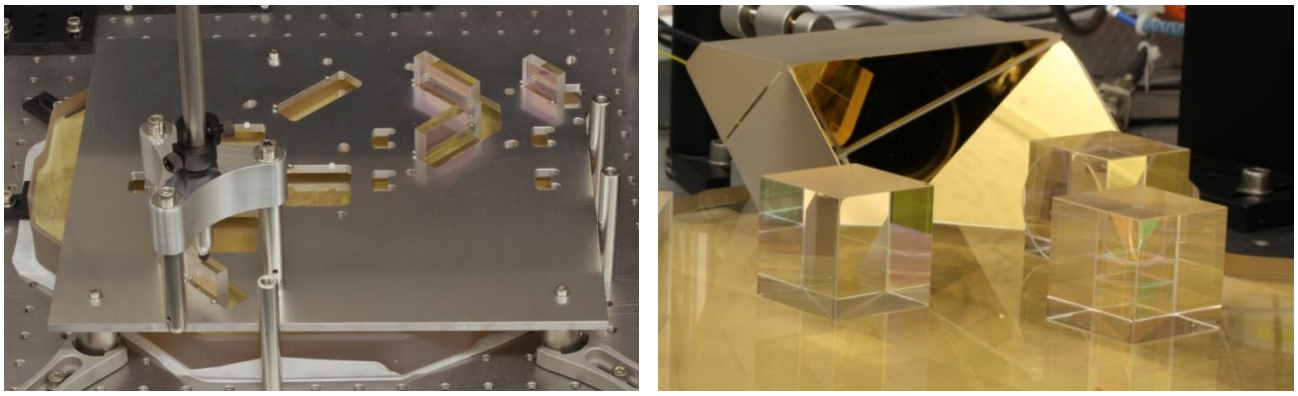

Figure 3, Positioning template for noncritical components (left) and corner cube retroreflector already bonded to the Zerodur baseplate (right).

The last mirror within the measurement path, however, determines the anti-parallel alignment of the external beams and therefore requires an alignment accuracy of a few ten microradians. For this purpose, a fixture based on a two dimensional piezo platform has been developed, which controls the mirror position during adhesive curing (Figure 4). For closed loop control, the alignment was measured using a Shack-Hartmann wavefront sensor. Afterwards the steering mirror and fiber launcher have been aligned and mounted.

The integration of the pupil imaging system takes place component-by-component using a laser beam, a camera, and a wavefront sensor for proper alignment. After finding the correct position for a component, a small positioning guide is temporarily attached to the baseplate by means of vacuum clamping, providing a reference for the component. All of the lenses are fixed into a metal lens mount having three leaf springs with direct contact to its lateral surface. For alignment purposes a second part of the lens mount is bonded to the baseplate so that the translation and rotation of the lens is adjustable by means of peel-off shims in between the two parts. Figure 4 (right side) shows the current status of integration. Once the imaging systems are completed, a few waveplates, the 45° folding mirror, and the Invar feet will be mounted so that the instrument performance can be evaluated in the dedicated verification setup.

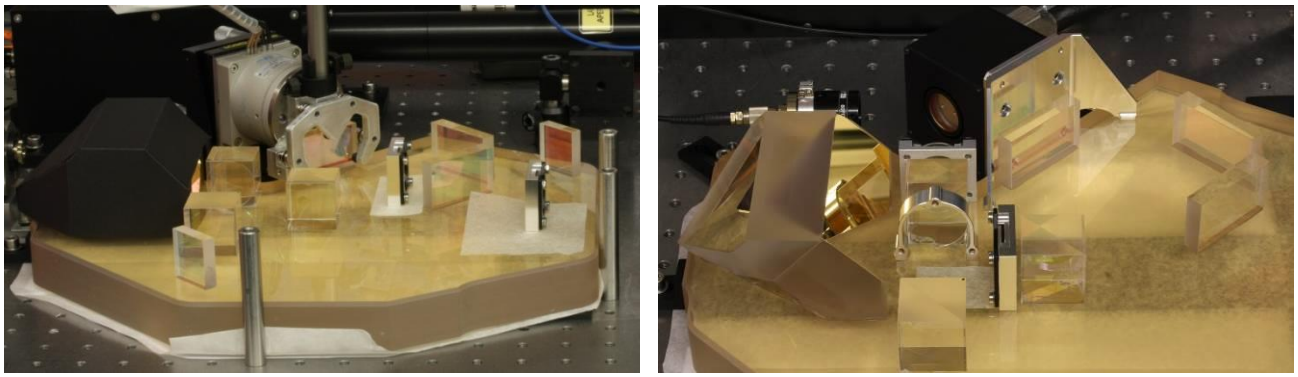

Figure 4, Piezo based integration of final mirror in closed loop control (left) and current status of integration (right).

3. EXPERIMENTAL PERFORMANCE VERIFICATION

After successful integration the optical instrument performance is evaluated during a measurement campaign performed using a dedicated test setup (OGSE). The achievable measurement accuracy is analyzed in terms of long-term stability and tilt-to-piston coupling. Therefore, a beam steering subsystem is included in the OGSE, which allows the measurement of pathlength variations while the angle of incidence at the optical instrument is changed. Four different laser beams are used during the measurements simultaneously, generating up to six distinct high-frequency beat notes. A field programmable gate array (FPGA) based digital signal processing unit provides frequency discrimination, phase evaluation and control of the beat signals from up to 20 photodiode channels. The optical design of the verification setup is depicted in Figure 5.

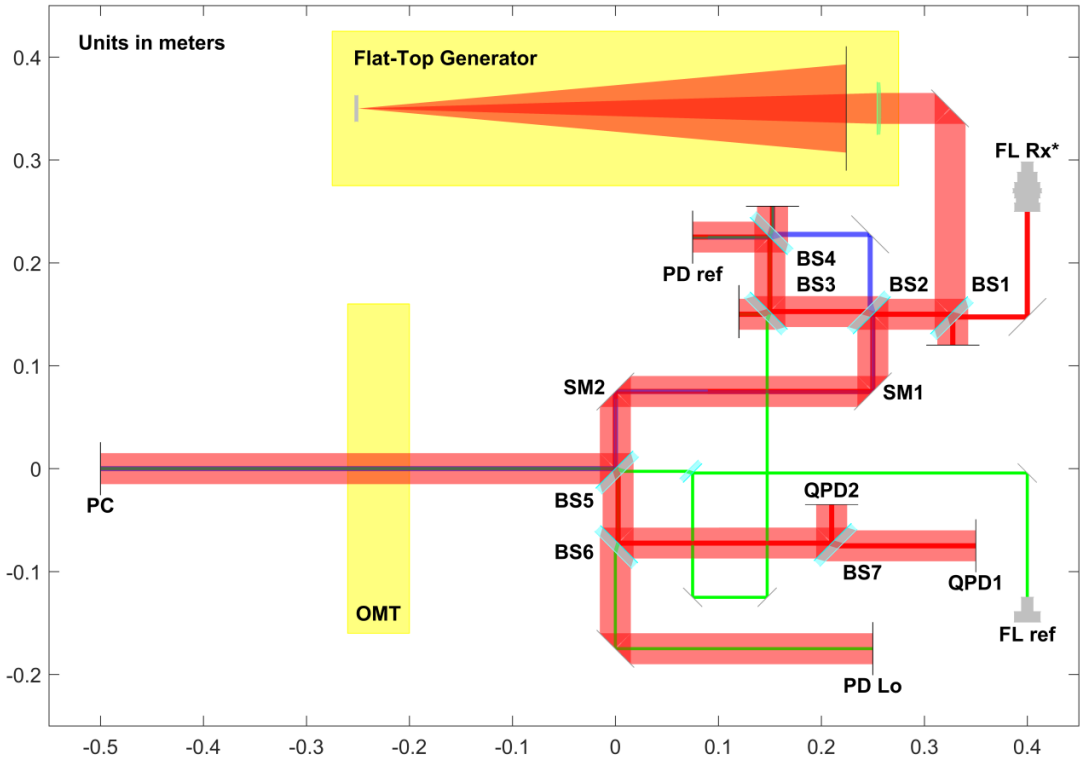

Figure 5, Scheme of the dedicated test setup for performance evaluation of the OMT regarding measurements of the long-term stability, tilt-to-piston coupling and initial signal acquisition. (FL - fiber launcher, BS - beam splitter, SM - steering mirror, PD - photodetector, QPD - quadrant photodetector, PC - phase center)

On one hand, the verification setup is the counterpart to the OMT in order to establish a laser link with valid photodiode signals on either side. On the other hand, the test setup provides additional features such as a flat-top beam generator, simulating the laser beam received from a distant spacecraft, and a reference path, which allows to monitor for pathlength variations introduced by the beam steering subsystem or thermal expansion within the test setup. A common 1064 nm Nd:YAG laser source will be used together with fiber-coupled acousto-optic modulators (AOMs) in order to generate four distinct laser beams. For advanced control capabilities e.g. phase locking and intensity stabilization, the AOM radio frequency input signals are connected to a FPGA based digital signal processing unit.

3.1 Flat-Top Laser Beam

For the experimental verification of the OMT, a flat-top generator has been designed and built, which serves as the received beam (Rx) for the OMT and is involved in all relevant pathlength measurements. Its flat wavefront and constant intensity profile imitate the properties of the laser beam received from the distant spacecraft. The practical realization is achieved with an apodized aperture [8], which adds a Gaussian intensity drop around a circular beam shape in order to minimize diffraction artefacts. The flat-top beam has an intensity drop-off of less than 3% within a 15 mm diameter and offers a wavefront quality much better than the other optical items ($\lambda/10$) used in the setup. The outer diameter of the beam profile is 30 mm, so that a 2" mirror size is sufficient. The laser source for the flat-top generator is the bare end of a single mode fiber. Due to the small fiber core, the beam has a divergency of about 5 deg and an almost perfect spherical wavefront. At a distance of 500 mm a single lens is used to collimate the wavefront. Directly in front of the lens the beam is clipped by the apodized aperture shown in Figure 6 (left). The four parameters of the aperture have been optimized using the simulated annealing algorithm and diffraction calculations. The aperture has been manufactured on a laser cutter out of copper sheet. Figure 6 also shows the simulated intensity profile (center) and the actual intensity of the flat-top beam generator (right). The working distance was optimized to be at 1 m with a depth of at least 40 cm.

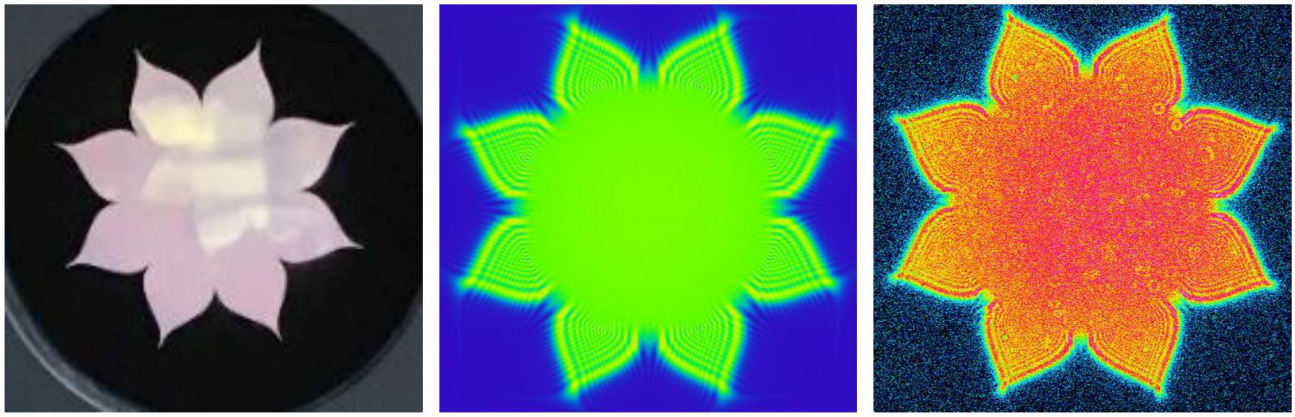

Figure 6, Apodized aperture, simulated intensity profile, and actual intensity profile of the flat-top generator

3.2 Beam Steering Subsystem

A part of the Rx beam arrives at the reference photodiode (PD ref, Figure 5) while another part is reflected at two motorized mirrors SM1 and SM2 before it enters the OMT. The output beam of the OMT (Tx, blue) is anti-parallel aligned to Rx and reflected at SM1 and SM2 as well. This means that the Tx beam position between SM1 and PD ref remains static regardless of the angle of incidence as long as the Rx beam is aligned to the reference point (PC). As a result, the corresponding beat notes at the QPD inside of the OMT and at PD ref contain all pathlength variations between BS2 and PC within its signal phase.

For a closed loop control of SM1 and SM2, the Rx beam position is measured by QPD1 and QPD2 (Figure 5). Since the Rx beam diameter exceeds the 5 mm diameter of the two QPDs and illuminates all quadrants identically the position of an additional smaller, superimposed Gaussian laser beam (Rx*) is measured instead. QPD1 is located at an optical copy of the Rx beam from PC, thus a direct measurement of the lateral beam offset can be made. The pathlength towards QPD2 is shorter so that the horizontal and vertical beam angle can be determined. The actuators SM1 and SM2 have an identical angular resolution but SM1 is causing a larger position offset at PC. As a consequence, SM1 is used to control

the position of the Rx beam and SM2 the angle respectively. This control scheme is applicable for piezo stepper driven actuators, since the total amount of drive pulses is minimized.

The beam steering subsystem has a significant impact on the pathlength between BS2 and PC, which will be measured by a reference interferometer. The reference laser beam (green, Figure 5) is superimposed in front of PD ref and PD Lo, another local optical copy of the Rx beam at PC. A pinhole in front of PD Lo will minimize the coupling of a relative tilt between the two beams into the beat signal amplitude. In conclusion, the tilt-to-piston effect of the OMT can be characterized after employing the aforementioned subsystems.

3.3 Phasemeter and Digital Signal Processing

All real-time tasks such as evaluation of the optical beat signals and calculation of the required control functions take place in the digital domain within a Xilinx Kintex UltraScale FPGA. The block diagram in Figure 7 gives an overview of the various interfaces between the FPGA and the other components of the experimental verification setup.

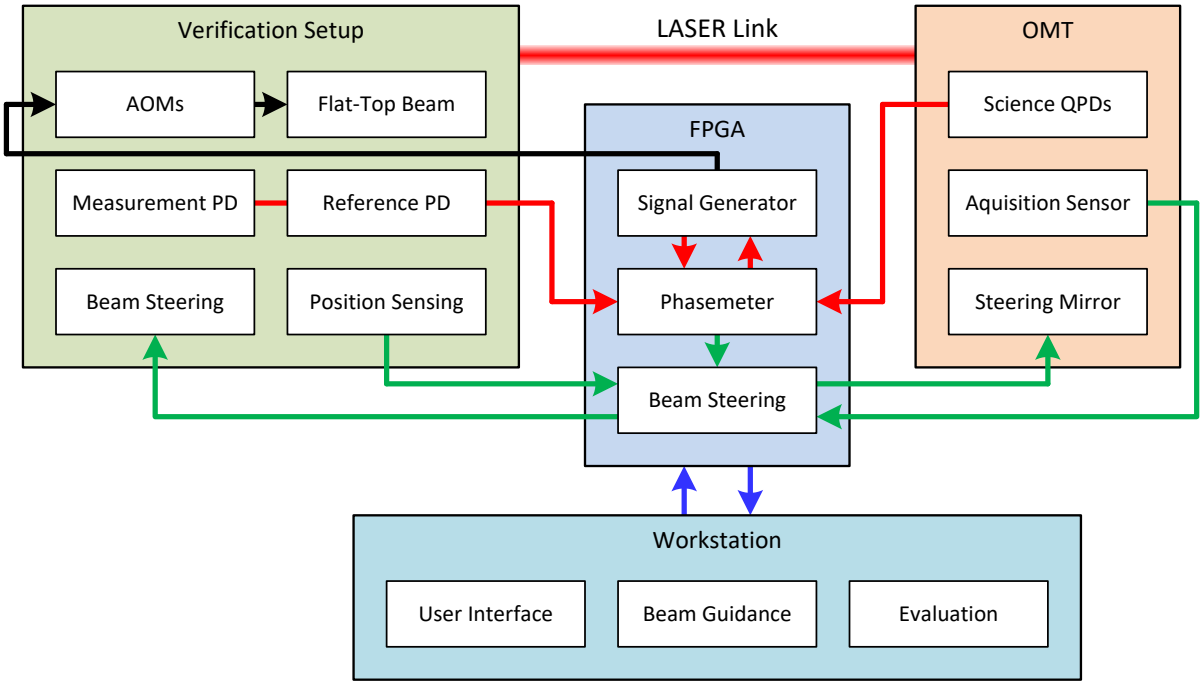

Figure 7, Block diagram of the various connections between the FPGA based digital signal processing system and the experimental verification setup.

A commercial PC821 PCIe FPGA board from Abaco Systems is used in the setup, equipped with FMC144 and FMC116 mezzanine cards providing the analog interfaces listed in Table 2. During measurements these interfaces produce a continuous data stream with a throughput of 8.5 GByte/s demanding real time computations. Up to six external devices such as lower frequency analog-to-digital converters (ADCs) and digital-to-analog converters (DACs) communicate directly with the FPGA via a custom interface board connected to the general purpose input/output header. All interfaces, including the mezzanine cards, are synchronized to a common external clock reference.

Table 2. Analog Interfaces of the FPGA based Signal Processing Unit

Unit	Direction	Resolution	Sampling Frequency	Application
FMC144	4x ADC	16-bit	370 MHz	Phasemeter input
	4x DAC	16-bit	1480 MHz (4x Interpolation)	AOM input signal
FMC116	16x ADC	14-bit	92.5 MHz	Phasemeter input
3x LTC2344	4x ADC	18-bit	86 kHz	Position sensing
STM32F103	16x ADC	12-bit	1 kHz	QPD DC readout
DAC8568	8x DAC	16-bit	156 kHz	Beam steering

The phasemeter is closely coupled to the AOM frequency generation subsystem. Four signal generators with advanced control capabilities regarding the signal amplitude and an infinitely adjustable phase offset are implemented in the FPGA and provide the high frequency signals for the AOMs. In addition the phase signals (without the phase offset) from all signal generators are subtracted from each other creating the reference for the phasemeter. The phase evaluation is based on an IQ-Demodulation scheme followed by a calculation of the arcus tangent, thus the relative phase between the input signal and the internal reference is measured at up to six frequencies simultaneously. The implementation of the arcus tangent is based on a CORDIC algorithm that computes both the phase difference and amplitude. All frequencies can be changed during runtime, however, a frequency spacing of at least 100 kHz between two beat notes offers adequate control bandwidth for phase locking and intensity stabilization, which takes place at PD ref. Since the regulators can directly access the phase and amplitude of the AOM signals, no further actuator is required.

While the demodulation happens at full sampling frequency, the arctangent is updated at a rate of 1 MHz. Phase readout for measurement signals in the sub-Hertz frequency band is provided by a cascaded integrator-comb decimation filter at a sampling frequency of 15 Hz. In order to still be able to track dynamic input signals and avoid cycle slips during actuation of the beam, a cycle counter is added to the phase value prior to decimation. Eventually the readout signal is sent to a computer for visualization, storage and post processing.

Furthermore the FPGA design includes position sensing and control loops for all motorized mirrors. Amplitude modulation in one of the AOM channels is used to distinguish the Gaussian Rx beam on QPD1 and QPD2 from any other beam and can also be used for the acquisition sensor to become less sensitive to straylight. Each of the photodiodes used for position sensing is connected to a custom amplifier board, which includes a LTC2344 4ch ADC. The FPGA acts as the master of the synchronous serial communication interface and calculates the horizontal and vertical position offset. The corresponding regulators generate the waveforms required by the piezo stepper actuators of the beam steering subsystem and send them to a DAC8568 8ch DAC, which is built into a rack providing six high voltage piezo drivers and two low voltage control signals for the OMT steering mirror. The parameters of the regulators as well as the set-points can be changed on the fly, offering the ability to steer the beam along arbitrary and complex tracks without changing the FPGA design. So far, the digital signal processing chain is fully implemented in the FPGA and is partially tested with synthetic signals.

The current state of the entire experimental setup is depicted in Figure 8. Once filly assembled, the OMT on the left side of the verification setup is raised into its final orientation perpendicular to the optical table. On top of the verification setup, the laser beam is distributed into four beams with adjustable signal power and connected to the fiber launchers by means of fiber coupled AOMs.

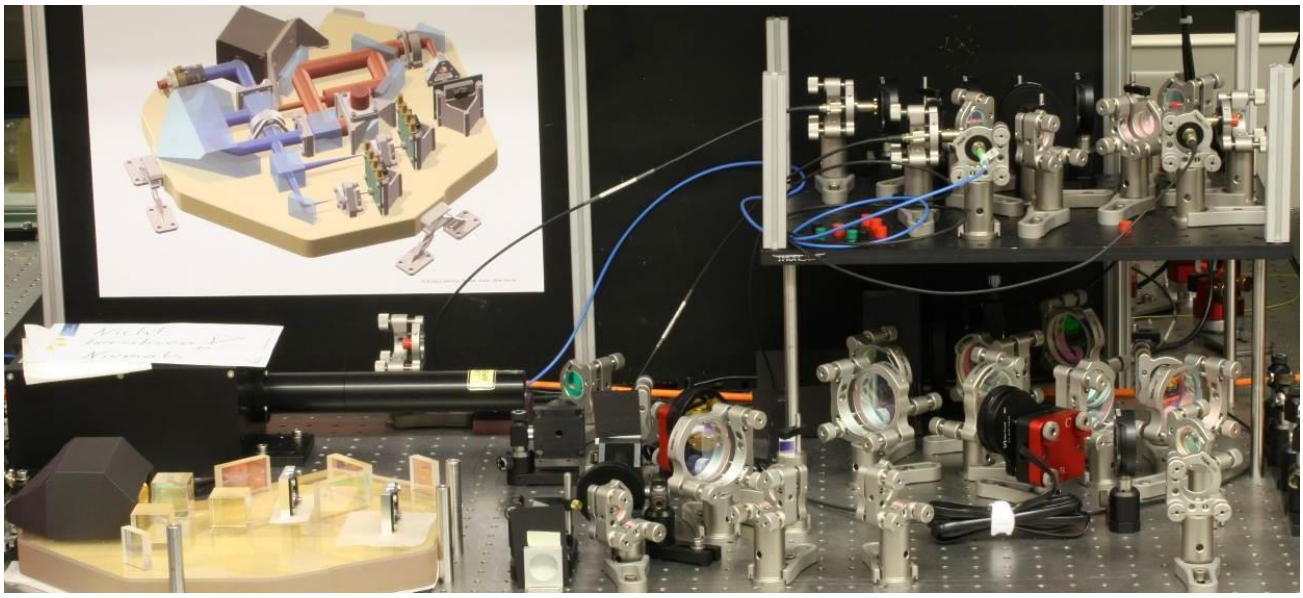

Figure 8, Photography of the experimental setup.

CONCLUSIONS

A dynamic laser ranging instrument is presented, which features the inherent beam tracking capabilities of a retroreflector with nanometer accuracy and a mono-axial output beam configuration to be used in a future gravity mission. The compact optical instrument will simplify spacecraft accommodation due to its flexible reference point location. An elegant breadboard is currently being integrated on a single, compact Zerodur baseplate for experimental verification. Once the instrument is fully assembled, the measurement performance will be evaluated in terms of long-term stability and tilt-to-piston coupling. A dedicated verification setup provides a flat-top beam generator simulating the laser beam received from a distant spacecraft and a beam steering subsystem which allows the measurement of pathlength variations while the angle of incidence at the optical instrument is changed. Further utilization of the instrument for laser communication or absolute distance measurements is subject to subsequent investigations.

ACKNOWLEDGEMENTS

Financial support by the German Aerospace Center (DLR) with funds provided by the Federal Ministry for Economic Affairs and Energy (BMWi) under grant numbers 50EE1407 and 50EE1409 is highly appreciated.

REFERENCES

[1] Sheard, B. et al., "Intersatellite laser ranging instrument for the GRACE follow-on mission," Journal of Geodesy, 86(12), 1083-1095 (2012).
[2] "e.motion – Earth System Mass Transport Mission. Proposal for earth explorer opportunity mission EE-8," Nansen Environmental and Remote Sensing Center (NERSC), Bergen, Norway, (2010).
[3] NGGM-D Team, "e2.motion - Earth System Mass Transport Mission (Square) - Concept for a Next Generation Gravity Field Mission," Deutsche Geodätische Kommission, Series B, vol. 2014, no. 318 (2014).
[4] NG2 team, "Assessment of a Next Generation Gravity Mission to Monitor the Variations of Earth's Gravity Field," Final report NG2-ASG-FR, Astrium GmbH, Friedrichshafen (2010).
[5] Mandel, O., Weise, D. and Chwalla, M., "Reflective device for use in an optical measuring system," U.S. Patent Application No. 15/485,894 (2017).
[6] Morrison, E. et al., "Automatic alignment of optical interferometers," Appl. Opt. 33(22), 5041–5049 (1994).
[7] Ressel, S. et al., "Ultrastable assembly and integration technology for ground-and space-based optical systems," Appl. Opt 49(22), 4296-4303 (2010).
[8] Cash, W., "Detection of Earth-like planets around nearby stars using a petal-shaped occulter," Nature, 442(7098), 51 (2006).